


# Impact of small-scale emerging flux from the photosphere to the corona: a case study from IRIS

Salvo L. Guglielmino<sup>1</sup> , Peter R. Young<sup>2,3,4</sup>, Francesca Zuccarello<sup>1</sup>, Paolo Romano<sup>5</sup> and Mariarita Murabito<sup>6</sup>

<sup>1</sup>Dipartimento di Fisica e Astronomia “Ettore Majorana” – Sezione Astrofisica,  
Università degli Studi di Catania,  
Via S. Sofia 78, 95123, Catania, Italy  
email: [salvatore.guglielmino@inaf.it](mailto:salvatore.guglielmino@inaf.it)

<sup>2</sup>Code 671, NASA Goddard Space Flight Center,  
Greenbelt, MD 20771, USA

<sup>3</sup>College of Science, George Mason University,  
Fairfax, VA 22030, USA

<sup>4</sup>Northumbria University,  
Newcastle upon Tyne, NE1 8ST, United Kingdom

<sup>5</sup>INAF – Osservatorio Astrofisico di Catania,  
Via S. Sofia 78, 95123 Catania, Italy

<sup>6</sup>INAF – Osservatorio Astronomico di Roma,  
via Frascati 33, I-00078 Monte Porzio Catone, Italy

**Abstract.** We report on multi-wavelength ultraviolet (UV) high-resolution observations taken with the *IRIS* satellite during the emergence phase of an emerging flux region embedded in the unipolar plage of active region NOAA 12529. These data are complemented by measurements taken with the spectropolarimeter aboard the *Hinode* satellite and by observations from *SDO*. In the photosphere, we observe the appearance of opposite emerging polarities, separating from each other, and cancellation with a pre-existing flux concentration of the plage. In the upper atmospheric layers, recurrent brightenings resembling UV bursts, with counterparts in all UV/EUV filtergrams, are identified in the EFR site. In addition, plasma ejections are observed at chromospheric level. Most important, we unravel a signature of plasma heated up to 1 MK detecting Fe XII emission in the core of the brightening sites. Comparing these findings with previous observations and numerical models, we suggest evidence of several long-lasting, small-scale magnetic reconnection episodes between the new bipolar EFR and the ambient field.

**Keywords.** Sun: magnetic fields, Sun: photosphere, Sun: chromosphere, Sun: transition region, Sun: corona, Sun: UV radiation

---

## 1. Introduction

A decade of observations of small-scale emerging flux regions (EFRs) in the solar atmosphere, carried out with increasing spatial resolution, has reinforced the idea that magnetic reconnection is likely to occur when the newly emerging magnetic flux interacts with the pre-existing ambient fields (e.g., [Guglielmino \*et al.\* 2010](#), [Ortiz \*et al.\* 2014, 2016](#), [Toriumi \*et al.\* 2017](#)). This process results in energy release, which is able to heat the upper atmospheric layers and to drive high-temperature plasma flows, according to early models

(Shibata *et al.* 1989, Yokoyama & Shibata 1995) and more recent numerical simulations (e.g., MacTaggart *et al.* 2015, Archontis & Syntelis 2019, Isliker *et al.* 2019).

In this context, observations performed by the Interface Region Imaging Spectrograph (*IRIS*, De Pontieu *et al.* 2014) satellite have revealed the presence of intense, small-scale ( $\approx 500 - 1000$  km), short-lived ( $\sim 5$  minutes) brightenings seen in ultraviolet (UV) images, called *IRIS* bombs (Peter *et al.* 2014) or UV bursts (Young *et al.* 2018). They are associated with opposite-polarity magnetic flux patches in the photosphere and seem to be caused by small-scale magnetic reconnection occurring in the low atmosphere.

Here, we describe a long-lived UV burst, which was observed in active region NOAA 12529 and showed a significant impact at coronal heights (Guglielmino *et al.* 2018, 2019).

## 2. Observations

Active region NOAA 12529 was observed in April 2016 (Fig. 1). It passed at the central solar meridian between April 13 and 14, being located at heliocentric angle  $\mu \approx 0.96$ . At that time, an EFR was emerging in the plage of the trailing polarity of the active region (see the solid box in Fig. 1).

During the EFR evolution, the *IRIS* satellite acquired an observing sequence between 22:34 UT on April 13 and 01:55 UT on April 14. This sequence consists of six large dense 64-step raster scans, covering a field of view of  $22'' \times 128''$  (see the dashed box in Fig. 1). UV observations included spectra of the C II 1334.5 Å and 1335.7 Å, Si IV 1394 and 1402 Å, Mg II k 2796.3 and h 2803.5 Å lines, as well as of other faint lines around the chromospheric O I 1355.6 Å line, comprising the coronal forbidden Fe XII 1349.4 Å line. The duration of each scan was about 33 minutes, with a 31.5 s step cadence and  $0.''33$  step size. Simultaneous slit-jaw (SJ) images were acquired in the 1400 (Si IV 1402 Å) and 2796 Å (Mg II k) passbands. These SJ images have a cadence of 63 s for consecutive frames in each passband, covering a field of view of  $144'' \times 128''$ . Further information about this *IRIS* data set can be found in Guglielmino *et al.* (2018).

We used full-disk continuum filtergrams and line-of-sight magnetograms, taken along the Fe I 6173 Å line by the Helioseismic and Magnetic Imager (HMI) on board the *SDO* satellite, to study the photospheric configuration of the EFR. Coronal images acquired by the Atmospheric Imaging Assembly (AIA) in the UV/EUV channels were also considered in this analysis. Moreover, observations acquired by the *Hinode* spectropolarimeter were used to determine the fine structure of the EFR in the photosphere.

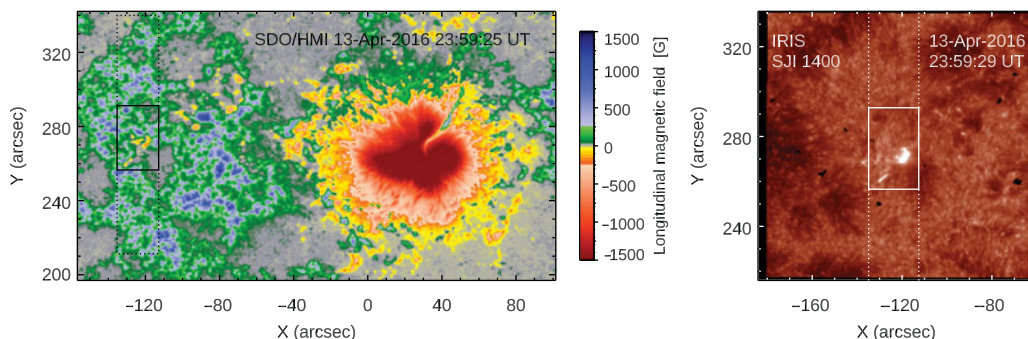


**Figure 1.** *Left panel:* Active region NOAA 12529 as seen in the *SDO*/HMI magnetogram. *Right panel:* Simultaneous *IRIS* SJ image in the 1400 Å passband. The solid-line box frames the EFR analyzed in the text. The dashed-line box indicates the area scanned by the *IRIS* slit.

### 3. Results

The analysis of the photospheric evolution of the EFR from *SDO*/HMI indicates that it emerged in a unipolar plage, where pre-existing flux concentrations were harbored, corresponding to pores in continuum images. In particular, the negative flux patch of the EFR approached a positive polarity pore that became smaller and finally disappeared, while the emerging magnetic flux formed a new pore with negative polarity.

At the flux peak, *Hinode* measurements show a mixed polarity pattern in the emergence zone, suggesting a serpentine magnetic field structure. In this region, elongated granules in the continuum as well as enhanced linear polarization signals were also observed.

During the three hours of the *IRIS* observing sequence, recurrent UV brightenings were observed in the EFR site. Comparing *SDO*/HMI magnetograms to *IRIS* radiance maps (see Fig. 2), we found that the brightenings occurred near the contact region between the positive pre-existing polarity field and the new emerging flux patch with negative polarity. Surge-like ejections, with a length of about  $10''$ , were repeatedly observed close to the UV brightenings, in particular at chromospheric heights (O I, Mg II and C II lines in Fig. 2). These were also seen in transition region lines (e.g., Si IV line in Fig. 2), showing an asymmetric appearance between the blue and red wings of the lines, reminiscent of the dynamics of the ejection (see Fig. 2). All of the *SDO*/AIA channels exhibited a long-lasting counterpart of the event, as seen for instance in the the 193 Å channel (Fig. 2).

UV spectra in the brightening core revealed the presence of plasma components with different velocity, mostly blueshifted. Some spectral features, like the absence of the O IV lines and the Mg II triplet emission, suggest that the burst occurred at low atmospheric heights. Notably, we also detected Fe XII emission ( $\log T$  [K]= 6.2) in the brightening core. This indicates that plasma is locally heated up to 1 MK and that the enhancements seen in the *SDO*/AIA channels have a genuine coronal origin.

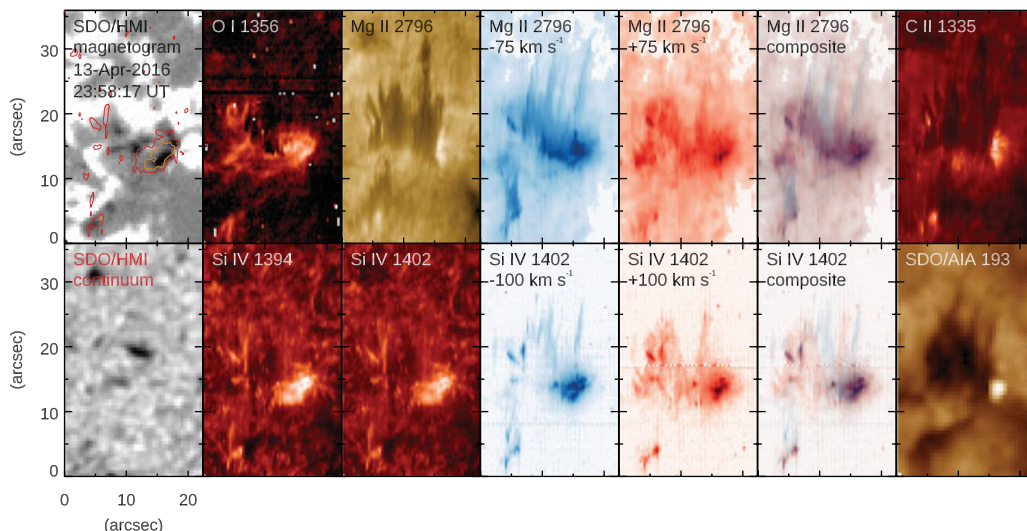


**Figure 2.** Synoptic view of the EFR at different atmospheric heights, during the third *IRIS* raster scan. The *SDO*/HMI magnetogram and continuum filtergram relevant to the half time of the *IRIS* scan are shown as a reference. Top panels display the morphology of the EFR in the chromosphere at increasing height. Bottom panels show the appearance of the EFR in the transition region, including a *SDO*/AIA filtergram in the 193 Å passband at the half time of the *IRIS* scan. For the chromospheric Mg II 2796 Å line and for the transition region Si IV 1402 Å line, we also show the morphology of the EFR in the blue and red wings of the lines.

#### 4. Implications

The analysis of this event strongly suggests that it is a result of magnetic reconnection between the emerging and the pre-existing field. Indeed, we find a general agreement of the evolution of the UV brightening with radiative magnetohydrodynamic numerical simulations concerning surges and UV bursts observed in flux emergence experiments (Nóbrega-Siverio *et al.* 2016, 2018). However, reconnection appears to occur at higher levels with respect to UV bursts, explaining the observed coronal counterpart.

We remark that the interaction between the pre-existing field and the new emerging flux is also important for the interpretation of larger events and greater amount of released energy (e.g., Romano *et al.* 2014), which might result in severe Space Weather phenomena (Zuccarello *et al.* 2013).

#### Acknowledgments

The research has received funding from the European Union's Horizon 2020 research and innovation programme under grant agreement nos. 739500 (PRE-EST project) and 824135 (SOLARNET project). This work was also supported by the Università degli Studi di Catania through the program: Piano per la Ricerca 2016-2018 - Linea di intervento 2 "Dotazione Ordinaria" and by the Space Weather Italian COmmunity (SWICO) Research Program. Support from INAF (National Institute for Astrophysics) – Catania Astrophysical Observatory is gratefully acknowledged. P.R.Y. acknowledges funding from NASA grant NNX15AF48G, and he thanks ISSI Bern for supporting the International Team Meeting "Solar UV Bursts – a New Insight to Magnetic Reconnection."

#### References

- Archontis, V. & Syntelis, P. 2019, *Philosophical Transactions of the Royal Society A*, 377, 20180387
- De Pontieu, B., Title, A. M., Lemen, J. R., *et al.* 2014, *Solar Physics*, 289, 2733
- Guglielmino, S. L., Bellot Rubio, L. R., Zuccarello, F., *et al.* 2010, *ApJ*, 724, 1083
- Guglielmino, S. L., Zuccarello, F., Young, P. R., Murabito, M., & Romano, P. 2018, *ApJ*, 856, 127
- Guglielmino, S. L., Young, P. R., & Zuccarello, F. 2019, *ApJ*, 871, 82
- Islaker, H., Archontis, V., & Vlahos, L. 2019, *ApJ*, 882, 57
- MacTaggart, D., Guglielmino, S. L., Haynes, A. L., Simitev, R., & Zuccarello, F. 2015, *A&A*, 576, A4
- Nóbrega-Siverio, D., Moreno-Insertis, F., & Martínez-Sykora, J. 2016, *ApJ*, 822, 18
- Nóbrega-Siverio, D., Moreno-Insertis, F., & Martínez-Sykora, J. 2018, *ApJ*, 858, 8
- Ortiz, A., Bellot Rubio, L. R., Hansteen, V. H., de la Cruz Rodríguez, J., & Rouppe van der Voort, L. 2014, *ApJ*, 781, 126
- Ortiz, A., Hansteen, V. H., Bellot Rubio, L. R., *et al.* 2016, *ApJ*, 825, 93
- Peter, H., Tian, H., Curdt, W. *et al.* 2014, *Science*, 346, 1255726
- Romano, P., Zuccarello, F. P., Guglielmino, S. L., & Zuccarello, F. 2014, *ApJ*, 794, 118
- Rouppe van der Voort, L., De Pontieu, B., Scharmer, G. B., *et al.* 2017, *ApJ Lett.*, 851, L6
- Shibata, K., Tajima, T., Steinolfson, R. S., & Matsumoto, R. 1989, *ApJ*, 345, 584
- Toriumi, S., Katsukawa, Y., & Cheung, M. C. M. 2017, *ApJ*, 836, 63
- Yokoyama, T. & Shibata, K. 1995, *Nature*, 375, 42
- Young, P. R., Tian, H., Peter, H., *et al.* 2018, *Space Science Reviews*, 214, 120
- Zuccarello, F., Balmaceda, L., Cessateur, G., *et al.* 2013, *Journal of Space Weather and Space Climate*, 3, A18